24th INTERNATIONAL CONGRESS ON SOUND AND VIBRATION
23–27 July 2017, London

THE FORMATION OF THE SPIRAL GAS-DYNAMIC FLOW IN THE FIELD OF STANDING ACOUSTIC WAVE

Anastasiya Gorbunova

Samara National Research University, 34 Moskovskoe sh., 443086 Samara, Russia,

Nonna Molevich

Lebedev Physical Institute, 221 Novo-Sadovaya Str., 443011 Samara, Russia,
Samara National Research University, 34 Moskovskoe sh., 443086 Samara, Russia,

Igor Zavershinskii

Samara National Research University, 34 Moskovskoe sh., 443086 Samara, Russia,

Dmitrii Zavershinskii

Lebedev Physical Institute, 221 Novo-Sadovaya Str., 443011 Samara, Russia,
Samara National Research University, 34 Moskovskoe sh., 443086 Samara, Russia,

The mechanism of formation of the experimemtally observed spiral structure of the discharge filament in a swirling flow is proposed. With the help of numerical simulation, the appearance of a spiral structure in an external flow is shown with the coincidence of the repetition rate of the discharge pulses with the fundamental acoustic frequency of the discharge tube.
Keywords: acoustic noise, vortex flow

1. Introduction

In [1], a possible mechanism for the formation of solitary spiral waves in the swirling flow in the presence of longitudinal plasmoid has been presented. The longitudinal plasmoid was created by a pulse repetitive capacity coupled HF discharge (CHFD) in the swirl argon flow at atmospheric pressure in a closed quartz tube [2]. The experimental study [2] showed that for pulse modulation with frequency range 850 - 875 Hz the plasma discharge structure transformed from a multifilament form to a single filament with a large loop traveling along the tube axis and rotating in the same time (Fig. 1). This frequency range is closed to the resonant frequency f_S of acoustic standing waves in tube $f_S = c_S / 2L \sim 870$ Hz (where L is the tube length, c_S is the sound speed in the argon flow heated by CHFD). So, it is reasonable to assume that the formation of this loop is associated with the CHFD excitation of a standing acoustic wave.

The proposed in [1] mechanism of spiral gas-dynamic structures forming involves the three-wave interaction between the standing acoustic wave and two bending modes of perturbed swirling flow with azimuthal wavenumbers $m = \pm 1$[3]. However, the estimations of parametric increment under conditions [2] lead to values that can't explain the appearance of a non-linear loop structure which matches the Hasimoto soliton [4,5].

In the present study, we have numerically simulated the gas-dynamic structure of the swirling flow under experimental conditions [2] and have proposed a model of the observed phenomena of acoustically induced formation of the spiral gas-dynamic flow structures.

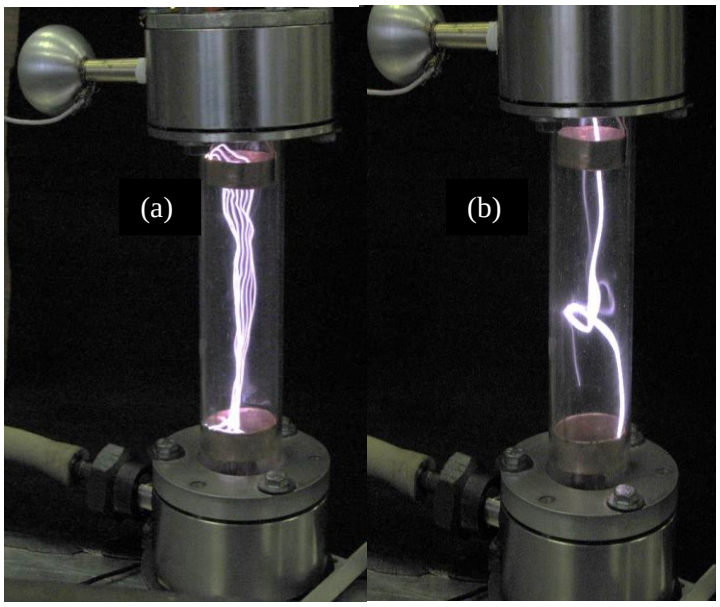

Figure 1: A longitudinal plasmoid created by pulse repetitive CHFD in the swirl flow. Multifilamental (a) and loop (b) forms [2].

2. Mathematical model and numerical procedure

For modelling the unsteady flow structure, we use the Reynolds averaged Navier-Stokes equations

$$\frac{\partial \rho}{\partial t} + \frac{\partial (\rho v_i)}{\partial x_i} = 0,$$

$$\frac{\partial (\rho v_i)}{\partial t} + \frac{\partial (\rho v_i v_j)}{\partial x_i} = -\frac{\partial P}{\partial x_i} + \frac{\partial}{\partial x_i}\left[\mu\left(\frac{\partial v_j}{\partial x_i} + \frac{\partial v_i}{\partial x_j} - \frac{2}{3}\delta_{ij}\frac{\partial v_k}{\partial x_k}\right)\right] + \frac{\partial}{\partial x_i}\left[-\rho\overline{v'_i v'_j}\right] + S_i(z,t), \qquad (1)$$

supplemented by the equations for energy and state

$$\frac{\partial (\rho E)}{\partial t} + \frac{\partial [v_i(\rho E + P)]}{\partial x_i} = \frac{\partial}{\partial x_j}\left[\left(\kappa + \frac{c_P \mu_t}{Pr_t}\right)\frac{\partial T}{\partial x_j} + v_i(\tau_{ij})_{eff}\right] + \Im(\vec{x}),\ P = \frac{\rho T}{M}, \qquad (2)$$

where $E = h - \frac{P}{\rho} + \frac{v^2}{2}$ and h are densities of total energy and enthalpy, respectively, $(\tau_{ij})_{eff} = \mu_{eff}\left(\frac{\partial v_j}{\partial x_i} + \frac{\partial v_i}{\partial x_j}\right) - \frac{2}{3}\mu_{eff}\frac{\partial v_k}{\partial x_k}\delta_{ij}$ is the deviatoric stress tensor, $\left[-\rho\overline{v'_i v'_j}\right]$ are Reynolds stresses, v_i, v'_i, ρ, T, and P are the mean and fluctuating velocity components, density, temperature and pressure, respectively, $\Im$ is the source power density, μ, μ_t, μ_{eff} are the molecular, turbulent, and effective viscosity coefficients, respectively, c_p is the molar specific heat capacity at constant pressure, κ is the thermal conductivity coefficient, Pr_t is the turbulent Prandtl number. The action of an external acoustic field was simulated by adding a source term $S_i(z,t)$ to the Navier-Stokes equations.

The non-dimensional parameters characterizing the flow are as follows:

$Re = \rho\langle v\rangle D/\mu$ is the Reynolds number, $S_n = G_t / RG_{ax}$ is the swirl number,

$Da = N / m_t c_P T$ is the Damköhler number. Here , $G_t = \int_0^R v_\varphi v_{ax} 2\pi r^2 dr$ is the axial flux of the tangential momentum, $G_{ax} = \int_0^R v_{ax}^2 2\pi r dr$ is the axial flux of the axial momentum,

where $\langle v \rangle = m_t / \pi R^2 \rho$ is the mass-averaged velocity, R and D are the radius and diameter of the tube, v_φ, v_{ax} are the tangential and axial velocities, respectively, N is the heat source power. Conditions [2] correspond to the Damköhler number $0.1 < Da < 1$ and Reynolds number $10^3 < Re < 10^4$. The swirl number $S_n < 1.5$ can be changed by varying of mass flow rates across the tangential and the axial inlets of the swirler.

We imposed the no-slip velocity and fixed temperature conditions along all tube walls and fixed mass flow conditions at the tube inlets. The inlet turbulent intensity is set to zero based on the experimental data [2]. At the outlet, we impose the pressure outlet boundary condition with the static pressure equal to the atmosphere pressure. The duct scheme and the description of experimental conditions [2] were presented in [1].

The numerical simulation of the swirling flow made using the ANSYS FLUENT program package, which solves the governing equations (1), (2) using the finite volume method. For spatial discretization of density, momentum, energy and turbulent quantities, a second-order upwind scheme is used. The diffusion terms are central-differenced and second-order accurate. The pressure values at the faces are interpolated by use of the second order scheme.

For transient terms, we use the fully implicit scheme of second-order accuracy. As a pressure-velocity coupling scheme, the SIMPLE method was used. The convergence was obtained when the residual reaches 10^{-6} for the energy equation and 10^{-4} for the continuity equation, the momentum equation, and the equations for turbulent quantities. The computational grid consists of $5.4 \cdot 10^5$ hexahedral cells. The grid refinement from $5.4 \cdot 10^5$ to $1.2 \cdot 10^6$ did not significantly alter the time-averaged velocity profiles.

3. Results of numerical simulation

Numerical simulation shows the presence of a non-stationary helical structure of the recirculation zone in the near-axis flow of the tube. The near-wall region corresponds to a direct flow (Fig. 2,3).

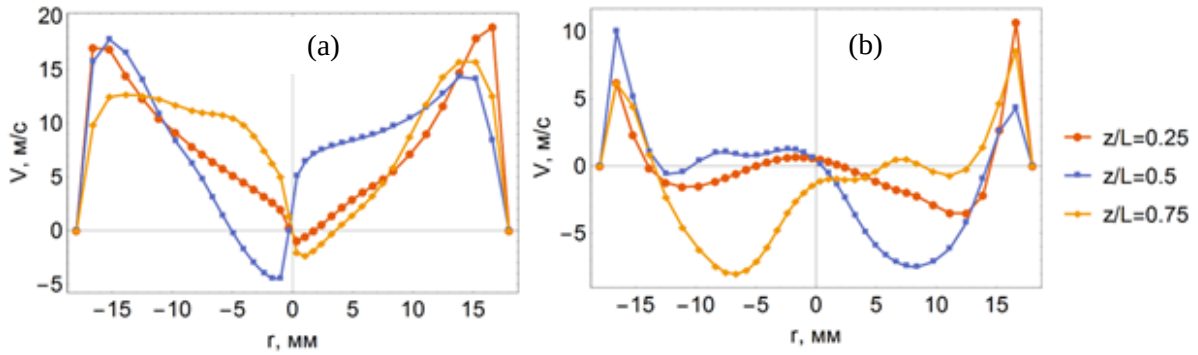

Figure 2: Profiles of tangential (a) and axial (b) velocities at different cross-sections. Mass flow rate m_φ = 1.5 g/sec. Heat source power N = 150 W.

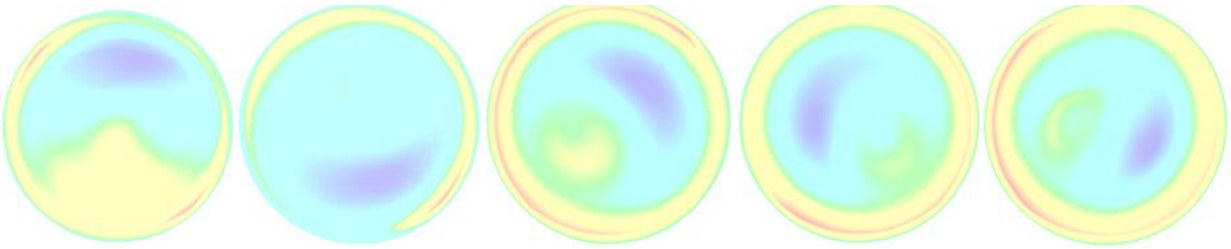

Figure 3: Axial velocity isolines in different cross-sections z = 1 cm, 5 cm, 10 cm, 15 cm and 18 cm obtained at a fixed time moment. The axial coordinate z increases left-to-right.

To visualize the flow structure the trajectories of test particles injected into the flow in the vicinity of the duct axis near the outlet are built (Fig. 4). It is clearly seen that the particles initially move in the opposite flow direction from outlet to inlet, rotating around the inner helix, then they pass to the outer near-wall region and move to outlet. In the absence of the sound wave and in non-resonant modes the particle lines are homogeneously distributed along the duct wall (Fig. 4(a)), whereas in the resonant mode the majority of particles passes an almost similar way while moving toward the outlet. These particles form a new spiral structure in the near-wall region (Fig. 4(b)). Comparing to the experimental results, one can suppose, that these spiral pathlines in an acoustic field produce a convective heat flux transferring heat from the hot inner discharge zone.

The physical mechanism of spiral flow formation is quite clear. The excitation of acoustic waves leads to appearing of the pressure gradient which is directed upstream in one wave phase and downstream at the another phase.

Therefore, at a small pressure gradient ΔP

$$|\Delta P| < \rho \frac{v_{ax}^2}{2}, \tag{3}$$

which can formed at non-resonant conditions or in the absence of acoustic field, particles always leaves the hot inner zone (Figs. 4(a), 5(a)). Here, v_{ax} is characteristic axial velocity in the inner zone.

At a significant pressure gradient directed against the direction of flow in the inner zone

$$|\Delta P| > \rho \frac{v_{ax}^2}{2}, \ \Delta P < 0, \tag{4}$$

which can formed at resonant conditions, particles do not leave the hot inner zone (Figs. 4(b), 5(b)).

Comparing to the experimental results (Fig. 1), one can suppose, that these spiral pathlines in an acoustic field produce a convective heat flux transferring heat from the hot inner discharge zone. The appearance of this flux leads to increase in the average ionization rate in the hot zones that leads to a significant drop in the resistance of the channel and forms a new discharge channel, whose shape follows the structure of the spiral flow.

However, the position of the discharge on the lower ring electrode varies randomly [1], so that the process of forming a new discharge channel does not occur continuously and is of a local nature. This can lead to the formation of a discharge region in the form of a solitary turn of a spiral propagating along the discharge tube, which qualitatively coincides with the type of evolution of the loop observed experimentally in [1] and close in form to the vortex soliton of Hashimoto [4,5].

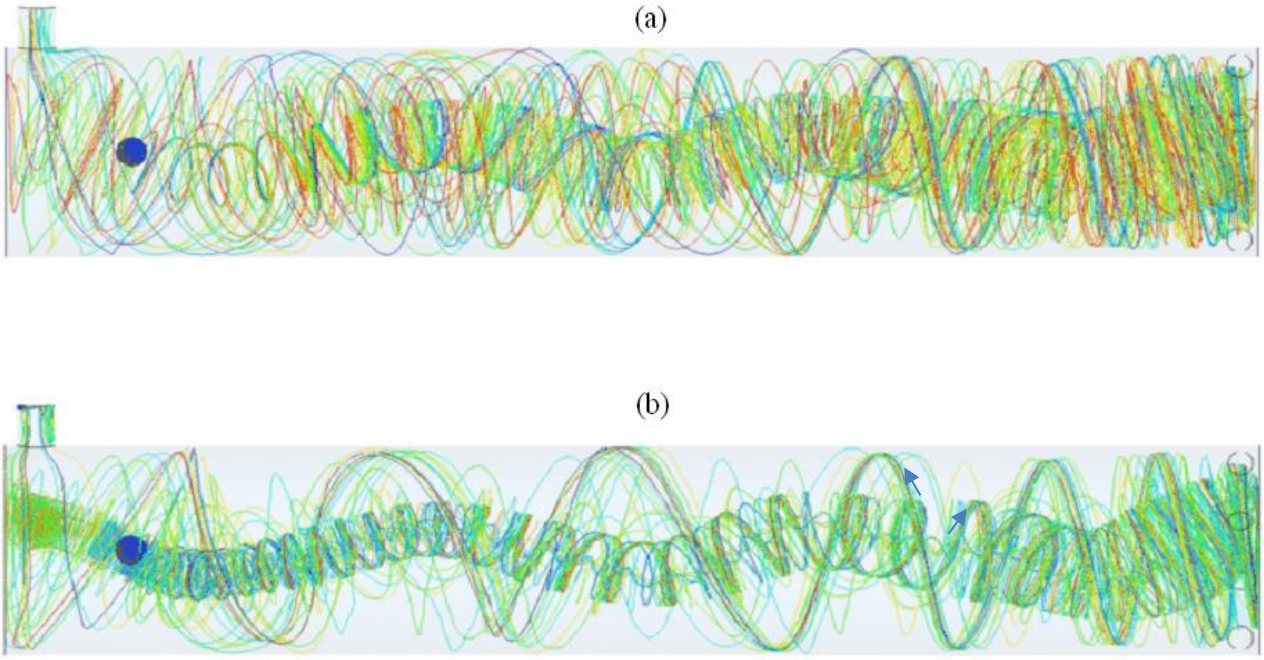

Figure 4: Particle trajectories at absence of acoustic noise or at non-resonant frequency (a) and at presence of acoustic noise of resonant frequency (b). The arrows show the flow directions in the inner and outer zones.

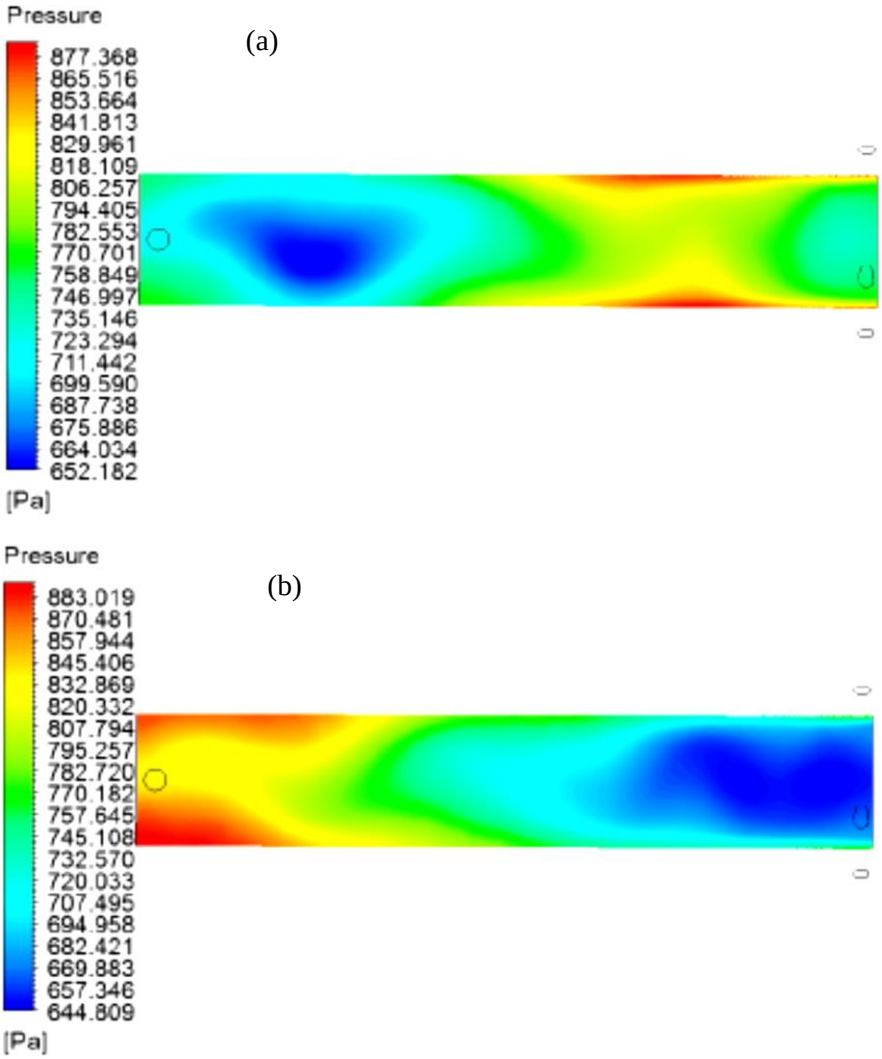

Figure 5: Pressure isolines at different phases of the standing acoustic wave of resonant frequency.

4. Conclusion

A mechanism of the experimentally observed helical disturbances of a plasma filament in swirling flows is presented. The numerical simulation of the gas flow shows that the acoustic standing wave forms a new helical structure in the near-wall tube region due to the appearance of a particular spiral trajectory, which is followed by majority of test particles. In the flow with a gas discharge, this pathline is supposed to carry the heat flux from the inner near-axis zone of discharge to the outer near-wall flow region. Heating of the gas flow causes an increase in the ionization rate and drop in the channel resistance that leads to the formation of a new discharge channel taking a helical shape of the gas flow pathlines. The shape of the simulated helical structure in the near-wall region can be matched with the experimentally observed large-amplitude disturbances of the plasma filament in the swirling flow with an excited standing acoustic wave.

The obtained vortex filament shape and its dependence on the parameters can be related to the so-called Hasimoto soliton [4,5]. Besides, the form of vortex line and its evolution during the motion are in qualitative coincidence with the experimentally observed behavior of vortex lines in a rotating tank [6] and in the conical vortex formed in the swirling flow in a conical diffuser [7].

5. Aknowlegements.

The study was supported supported by the Ministry of education and science of Russia under project 3.1158.2017 and by RFBR under grant 16-41-630591 r_a.

REFERENCES

1 Gorbunova, A., Molevich, N., Sugak, S., Zavershinskii, I. Hasimoto soliton on vortex cores in acoustic field, *Proceedings of the 23th International Congress on Sound and Vibration*, Athens, Greece, 10–14 July (2016).

2 Klimov, A. I. *et al.* Longitudinal Plasmoid in High-Speed Vortex Gas Flow Created by Capacity HF Discharge, Technical Report ISTC Project No. 3794P (2010).

3 Gorbunova, A., Klimov, A., Molevich, N., Moralev, I., Porfiriev, D., Sugak, S., Zavershinskii, I. Precessing vortex core in a swirling wake with heat release, *International Journal of Heat and Fluid Flow*, **59**, 100-108 (2016).

4 Hasimoto, H. A soliton on a vortex filament, *Journal of Fluid Mechanics*, **51** (03), 477–485 (1972).

5 Leibovich, S. and Ma, H. Y., Soliton propagation on vortex cores and the Hasimoto soliton, *Physics of Fluids*, **26** (11), 3173–3179 (1983).

6 Hopfinger, E. J., Browand, F. K., Gagne, D. Turbulence and waves in a rotating tank, *J. Fluid-Mech.*, **125**, 505-53 (1982).

7 Alekseenko, S. V., Kuibin, P. A., Shtork, S. I., Skripkin, S. G., Tsoy, M. A. Vortex reconnection in a swirling flow, *JETP Letters*, **103** (7), 455–459 (2016).